Behavioral/Cognitive

A Precuneal Causal Loop Mediates External and Internal Information Integration in the Human Brain

Dian Lyu,[1,2] Ioannis Pappas,[1,3] David K. Menon,[1,4] and Emmanuel A. Stamatakis[1,2]

[1]University Division of Anaesthesia, University of Cambridge, Addenbrooke's Hospital, Cambridge CB2 0SP, United Kingdom, [2]Department of Clinical Neuroscience, University of Cambridge, Addenbrooke's Hospital, Cambridge CB2 0SP, United Kingdom, [3]Helen Wills Neuroscience Institute, University of California, Berkeley, California 94720, and [4]Wolfson Brain Imaging Centre, University of Cambridge, Cambridge CB2 0QQ, United Kingdom

Human brains interpret external stimuli based on internal representations. One untested hypothesis is that the default-mode network (DMN), widely considered responsible for internally oriented cognition, can decode external information. Here, we posit that the unique structural and functional fingerprint of the precuneus (PCu) supports a prominent role for the posterior part of the DMN in this process. By analyzing the imaging data of 100 participants performing two attention-demanding tasks, we found that the PCu is functionally divided into dorsal and ventral subdivisions. We then conducted a comprehensive examination of their connectivity profiles and found that at rest, both the ventral PCu (vPCu) and dorsal PCu (dPCu) are mainly connected with the DMN but also are differentially connected with internally oriented networks (IoN) and externally oriented networks (EoN). During tasks, the double associations between the v/dPCu and the IoN/EoN are correlated with task performance and can switch depending on cognitive demand. Furthermore, dynamic causal modeling (DCM) revealed that the strength and direction of the effective connectivity (EC) between v/dPCu is modulated by task difficulty in a manner potentially dictated by the balance of internal versus external cognitive demands. Our study provides evidence that the posterior medial part of the DMN may drive interactions between large-scale networks, potentially allowing access to stored representations for moment-to-moment interpretation of an ever-changing environment.

Key words: default-mode network; precuneus; large-scale networks; cognitive control

Significance Statement

The default-mode network (DMN) is widely known for its association with internalized thinking processes, e.g., spontaneous thoughts, which is the most interesting but least understood component in human consciousness. The precuneus (PCu), a posteromedial DMN hub, is thought to play a role in this, but a mechanistic explanation has not yet been established. In this study we found that the associations between ventral PCu (vPCu)/dorsal PCu (dPCu) subdivisions and internally oriented network (IoN)/externally oriented network (EoN) are flexibly modulated by cognitive demand and correlate with task performance. We further propose that the recurrent causal connectivity between the ventral and dorsal PCu supports conscious processing by constantly interpreting external information based on an internal model, meanwhile updating the internal model with the incoming information.

Introduction

The intrinsic coupling [or functional connectivity (FC)] between regions in the human brain is not random but rather forms consistent spatial patterns known as intrinsic (functional) connectivity networks (ICNs; Seeley et al., 2007). Each ICN's relevance to cognitive function has been established from activation studies, from which we can infer what information features are encoded in different networks (Cole et al., 2014). Interactions between ICNs are thought to be a form of information exchange serving cognitive demands, although the precise functional role of those interactions remains an active area of research (Bressler and Menon, 2010). A case in point is the interaction between the default-mode network (DMN) and cognitive control networks which have been reported to be anticorrelated (Fox et al., 2005) and contraposed in their cognitive function (Weissman et al., 2006). This view however is increasingly challenged by accumulating

Received Mar. 28, 2021; revised Aug. 29, 2021; accepted Sep. 14, 2021.

Author contributions: D.L., D.K.M., and E.A.S. designed research; D.L., I.P., and E.A.S. performed research; D.L. and E.A.S. analyzed data; D.L. wrote the first draft of the paper; D.L., I.P., D.K.M., and E.A.S. edited the paper; D.L., I.P., and E.A.S. wrote the paper.

Data provided, in part, by the Human Connectome Project, WU-Minn Consortium (Principle Investigators: David Van Essen and Kâmil Uğurbil; 1U54MH091657) was supported by the National Institutes of Health (NIH). This work was supported by the NIH blueprint for Neuroscience Research and by the McDonnell Center for Systems Neuroscience at Washington University. This work was supported by grants from the Cambridge Trust in partnership with China Scholarship Council (to D.L.); the Oon Khye Beng Ch'Hia Tsio Studentship for Research in Preventive Medicine, Downing College, University of Cambridge (to I.P.); the Canadian Institute for Advanced Research (CIFAR) (to D.K.M. and E.A.S.); The National Institute for Health Research (NIHR, UK), Cambridge Biomedical Research Centre and NIHR Senior Investigator Awards (to D.K.M.); The British Oxygen Professorship of the Royal College of Anaesthetists (to D.K.M.); The Stephen Erskine Fellowship, Queens' College, University of Cambridge (to E.A.S.). Computing infrastructure at the WBIC High Performance Hub for Clinical Informatics was funded by Medical Research Council research infrastructure Award No. MR/M009041/1.

The authors declare no competing financial interests.

Correspondence should be addressed to Emmanuel A. Stamatakis at eas46@cam.ac.uk.

https://doi.org/10.1523/JNEUROSCI.0647-21.2021

findings. While the majority of DMN studies focus on resting state, i.e., data collected in the absence of external stimulation, emerging evidence shows that the DMN is indeed engaged during goal-directed tasks (Spreng et al., 2014; Elton and Gao, 2015; Vatansever et al., 2015), as opposed to being a "resting-state" network.

Conscious processing, whether externally oriented or not, always entails some form of internal processing. A dominant theory of consciousness, predictive coding, has provided a more realistic Bayesian model to explain brain function, which postulates that the external physical world is never faithfully represented in our brains, but rather through a filter of our internal belief of the world (Friston and Kiebel, 2009; Friston, 2012; Barrett and Simmons, 2015; Allen and Friston, 2018). Motivated by pharmacological and brain injury studies that highlight the DMN's prominent role in conscious processing (Vanhaudenhuyse et al., 2010; Liu et al., 2015; Perri et al., 2016), we hypothesized that the DMN is fundamental when considering the neural instantiation of such an account, given its multifaceted role in external and internal processing.

The DMN, which comprises medial frontal and medial posterior parietal cortices as well as the angular gyrus (AnG) and hippocampus, is neither anatomically nor functionally homogeneous (Kernbach et al., 2018). Among the DMN regions, the posteromedial cortex (PCu/PCC) has attracted significant interest because of its complex neuroanatomical, metabolic and functional fingerprint (de Pasquale et al., 2012; Raichle, 2015). It has exceptionally high metabolic rate (Raichle et al., 2001) and also is a major connectivity hub from a graph-theoretic perspective (van den Heuvel and Sporns, 2011; Tomasi and Volkow, 2011; Demertzi et al., 2013). The precuneus (PCu) has been characterized as the inter-network nexus within the DMN, for its connectivity with the DMN and the frontoparietal control network (FPCN) which is distinct between rest and task states (Utevsky et al., 2014). Based on its functional features we hypothesized that the PCu may play a key role in integrating external information with internal representations such as episodic memory, self-related information and subjective values that are processed by other DMN regions.

In fact, the PCu is engaged in such a broad range of cognitive tasks (including both internally and externally oriented, goal-directed tasks) leading some to suggest that it is not part of the DMN (Fletcher et al., 1995; Cavanna and Trimble, 2006). However, the task-positive subregion of the PCu has been found to have higher intrinsic FC with the DMN than with the FPCN (Utevsky et al., 2014). To investigate the network associations of the PCu during tasks, we first ascertained its involvement in cognitive tasks by employing a *NeuroSynth* meta-analytic framework (Yarkoni et al., 2011). We then used multiple MRI datasets [diffusion MRI (dMRI), resting-state and task-state fMRI] from the Human Connectome Project (HCP) to investigate the activation, functional and structural connectivity (SC) of the PCu. We found that the ventral PCu (vPCu) and dorsal PCu (dPCu) subdivisions had distinct activation and connectivity patterns, which followed the spatial patterns of internally oriented networks (IoN)/externally oriented networks (EoN), suggesting that the PCu might mediate the integration between internally and externally oriented cognitive processes. Moreover, dynamic causal modeling (DCM) provided evidence for the directed coupling between the two PCu subdivisions which was modulated by task difficulty, hinting at a combinatorial processing mode where incoming information is associated with internal representations.

Materials and Methods

NeuroSynth meta-analysis of fMRI studies

When this work was conducted, the *NeuroSynth* database contained 14,371 neuroimaging studies (https://github.com/neurosynth/neurosynth-data), associated with >3200 text-based features and over 410,000 activation peaks that span a wide range of published neuroimaging studies. Since our focus is DMN functionality during tasks we searched for activation coordinates associated with attentional and executive tasks. These were generated by interrogating the database with the text-based search: "attention* or execut*." Both forward and reverse inferences were performed to assess both necessity and sufficiency of a region's response to a certain type of task. Specifically, the forward-inference search relies on the probability of observing activation given the presence of the term [i.e., $P(Activation|Term)$], thus essentially testing the consistency of a region's activation to a type of task. On the other hand, reverse inference relies on the probability of the specified term being frequently discussed alongside a specific activation [i.e., $P(Term|Activation)$], thus revealing the regions that are selectively associated with the term. Key parameters were based on the default values in the publicly available *NeuroSynth* toolbox (https://github.com/neurosynth/neurosynth). For example, a frequency cutoff of 0.001 for article words was used to determine whether a study used the term incidentally or purposely. Resulting activation was false discovery rate (FDR)-corrected for multiple comparisons using a whole-brain FDR threshold of 0.01 at the voxel level. This generated Z score maps with values generally bigger than 3. For a better visualization of the result, we used a cutoff of $Z = 4$ to only show bigger clusters.

fMRI and diffusion-weighted data analyses

Participants

We utilized the multimodal MRI data from HCP dataset released in March 2017. The data of "100 unrelated" participants were downloaded, including structural, diffusion MRI (dMRI) data and fMRI data of the resting state and two classic cognitive tasks. All the participants are young healthy adults between the ages of 22 and 35, with no documented history of psychiatric, neurologic, or medical disorders known to influence brain function. For a complete description of inclusion and exclusion criteria for the HCP datasets, please see the original publications for additional details (Van Essen et al., 2012, 2013; Barch et al., 2013).

Selected tasks

We selected the relational processing (RP) task and the N-back working memory (N-back) task from the HCP, as these have two levels of difficulty, therefore affording the possibility to infer the brain's response to varying cognitive demand. Task-related analyses for the two tasks were conducted independently for each task. In the main text, domain-specific terms indicating a certain level of specific cognitive demand (such as 0-back and 2-back in the N-back task) were substituted with the general terms of "easy" and "difficult" to indicate the load of general cognitive abilities.

Image preprocessing

The ready-to-use HCP data have already been minimally preprocessed and quality-checked by the distributors (Glasser et al., 2013) and we conducted extra preprocessing steps with SPM12 (https://www.fil.ion.ucl.ac.uk/spm/). Specifically, the data were smoothed with a Gaussian kernel of 6-mm full-width half maximum (FWHM) and no low-pass filtering was used as it might reduce signal strength and sensitivity. No global signal regression was used, for it may cause anticorrelation artifacts by shifting the distribution of FC toward negative values (Murphy et al., 2009; Chai et al., 2012). To reduce the influence of non-neuronal confounds, eigenvalues were extracted from blood oxygen level-dependent (BOLD) signals within CSF and white matter template masks and were regressed out from target signals during statistical testing.

Activation studies

Whole-brain activation was estimated using the standard SPM general linear model (GLM) approach. For the individual-level GLM, the main regressors for task effect were constructed by convolving the

hemodynamic response function (HRF) which codes the BOLD signal, with the event-related boxcar function which codes the sustained brain activation from a stimulus onset to a motor response (for correctly responded trials). The main effects of the two conditions, i.e., difficult (2-back or relational) and easy (0-back or match) conditions, were modeled as different regressors. Covariates of the non-neuronal nuisance such as the signals from CSF and white matter, block effects and 6 movement regressors were also specified to be regressed out. Based on the GLM, contrasts of difficult > easy and of easy > difficult were used to reveal activated and deactivated regions. Group-level GLMs were then constructed to test the significance of the brain activation in the population level, with age and sex as covariates.

Selection of regions of interest (ROIs)

We were interested in the functionality of the PCu during attentional demanding goal-directed tasks; therefore, ROIs were selected based on our activation results from the N-back and RP tasks. Both activated and deactivated PCu regions associated with increased level of difficulty of the tasks were considered. To ensure the PCu region that we are considering is actually part of the DMN, we also superimposed it on the DMN canonical mask as defined by the Conn network atlas (Whitfield-Gabrieli and Nieto-Castanon, 2012). The seed regions were selected by computing the spatial intersection of (1) the significant cluster (exceeding the cluster-level family wise error (FWE)-corrected p of 0.05) from activation contrasts in the task; (2) the PCu as defined by the regional atlases (i.e., Oxford-Harvard cortical atlases) implemented in the Conn toolbox (https://www.nitrc.org/frs/shownotes.php?release_id=2823); and (3) the DMN spatial localization identified by the Conn network atlas. For task-state and task-related FC (tsFC and trFC) analyses which were conducted independently for each task, the seeds were generated independently for the N-back and the RP task, given their activation profiles in the corresponding task. Timeseries (i.e., the first eigenvectors) were extracted from seed regions during the course of the experiment for each of the tasks. When task data were not used, i.e., for SC and resting-state FC (rsFC) analyses, the spatial localization of the seeds was confined by the common activation between the two tasks; hence, the seeds were constructed by computing the overlap between the PCu seeds from the two tasks.

Resting-state seed-based FC of v/dPCu

Using SPM12, we calculated the FC as the correlation coefficient from the GLM estimation. We used the timeseries (first eigenvector) extracted from the seed regions (v/dPCu) as the covariate to regress against the signals from the rest of the brain, while controlling for the effect of non-neuronal confounds (estimated from white matter and CSF) and head movements. Baseline FC and differences between the FC of the v/dPCu at the group level were estimated with one-sample and paired t tests.

SC of v/dPCu

The acquisition, preprocessing the dMRI images from the HCP and the generation of diffusion tensor maps has been detailed in published articles (Sotiropoulos et al., 2013). Based on the diffusion tensor images we built probabilistic tractography in FSL5 (https://fsl.fmrib.ox.ac.uk/fsl/fslwiki/FDT). The SC matrix for each individual was obtained using vPCu and dPCu as the seed and the gray matter as the termination mask. Each entry in the connectivity matrix stands for the number of streamlines (out of 5000) from each voxel of the seed map (vPCu or dPCu) that had a 50% chance or greater of reaching the gray matter (curvature threshold = 0.2), which was also corrected for the distance/length of the pathways. A seed's SC to the gray matter was calculated by averaging the streamline connections from all the voxels of the seed, which was then projected to a standard MNI brain space for further statistical parametric mapping analyses in SPM12. Similar to FC analyses, baseline and difference of the SC of the dPCu and vPCu at the group level were calculated with one-sample and paired t tests. The brain maps of the statistical parametric values for each ROI were then smoothed with a Gaussian kernel of 6-mm FWHM.

Task-state seed-based FC of v/dPCu

Task-state FC (tsFC) was derived based on partial correlations of the timeseries between the seed and the rest of the brain, after controlling for the effects of the event-related BOLD response (boxcar experiment design convolved with the canonical HRF; boxcar function was used for assuming sustained brain activation from the stimulus onset to motor reaction) weighted by contrasts, as well as other non-neuronal confounds (i.e., block effects, head movement regressors, CSF and WM timeseries) during the course of the experiment.

We measured the tsFC not only because it can provide additional information about functional coupling during tasks, but also because it can complement the subsequent psychophysiological interaction (PPI) analyses. The PPI measures relative changes of FC strength regardless of its baseline being negative or positive. This can cause ambiguity for understanding the PPI result especially when the FC of DMN regions is under investigation, since the DMN is widely known as being anticorrelated with task-associated regions. A simple solution is to measure the FC during tasks which serves as a FC baseline on which the task-induced modulation will have an effect on, then we can interpret the PPI results based on the valence of the FC.

However, a simple correlation of BOLD signals as measured in the resting state might not be appropriate, because on an input of a stimulus, there might be an increase of overall blood oxygenation in the relevant regions. The correlation of these regions would be a result driven by the third party, i.e., the external stimuli; rather than being directly correlated in their timeseries. Therefore, to establish the "true" FC during the period of task, we examined the partial correlation independent of event-related BOLD activation during the course of the experiment, which actually follows the same logic of the PPI modeling. Conveniently, the resulted positivity in the value of tsFC can further facilitate the interpretation of the task-induced modulations on the FC that will be measured in the subsequent PPI analysis.

PPIs

PPI was used to evaluate by what amount the cognitive variables during tasks upregulate or downregulate the FC between the seed region and its functionally coupled regions.

The implementation of the PPI was similar to the above seed-based FC during tasks, but additionally the GLM model included an interaction term, i.e., a new variable created by dot multiplying the HRF-convolved boxcar function associated with the task events and the seed's timeseries. Individual-level PPIs were estimated separately for the N-back and the RP task. As the PPI reveals the FC that can be modulated by the task variables, we called it trFC in this article.

We first conducted PPI analyses independently for the two tasks and we observed a common pattern of the trFC between the N-back and the RP tasks. We then focused on the common pattern by averaging the individual-level trFC between the two tasks, and we conducted another group inference based on the individual averaged β values.

The two tasks were considered together when examining the trFC's behavioral relevance. To do that, in the group-level GLM, the trFC measured by individual-level PPIs were modeled as the dependent variable, with the individuals' reaction time (RT) difference between two conditions as the main regressor, with the individuals' age, sex and task identity as covariates of no interest. As the two tasks were performed by a same group of people, the GLM effectively adopts a repeated-measure ANCOVA design, with "RT" and "tasks", respectively, as the continuous and categorical independent variables. As a result, the main effect of the RT was examined while being adjusted for the "session" effect (the data for the two tasks were acquired in different scanning sessions).

Anatomical labels and ICN identification based on significant clusters

To make inferences about the cognitive function of significant regions, we used the functionally defined ICN-BM network atlas (https://www.nitrc.org/projects/ICN_atlas/) for identifying the ICNs involved in the two tasks. The advantage of using the ICN-BM atlas was that the nomenclature used in the atlas not only corresponds to the well-known canonical resting-state connectivity networks, but also to task-based co-activation networks which were generated from a meta-analyses using

the BrainMap (BM) dataset (Smith et al., 2009; Cole et al., 2016). This robust correspondence between ICNs and cognitive functions allowed us to make inverse inferences, that is to infer implicit cognitive processes from engaged brain areas.

We used the MATLAB-based *ICN_atlas* toolbox to determine each significant cluster's region/ICN correspondence by rating their spatial overlaps with the predefined regions/ICNs (Smith et al., 2009; Laird et al., 2013; Cole et al., 2016; Ito et al., 2017; Kozák et al., 2017). When reporting the PPI result, we also applied the same strategy to establish the correspondence of the Conn atlas and the ICN-BM atlas for visualizing both the seed-based FC regions (defined by the Conn atlas) and the ICNs they belong to.

The spatial overlap reported in the main article was calculated as the ratio of the number of activated voxels over the region/ICN volume which the voxels belong to (Eq. 1; Kozák et al., 2017).

$$I_i = \frac{|SPM_t \cap ICN_i|}{|ICN_i|}. \quad (1)$$

Besides the activation maps and their associated ICN domains shown in the main text, we also report significance tables with detailed coordinates in the online repository: https://github.com/Aubrey-Lyu/data-analysis_Project_HCP_diffPCu/blob/main/group_results/Significance_tables.pdf. For identifying the anatomic regions based on the coordinates, we adopted the toolboxes of GingerALE (http://brainmap.org/ale/) and Talairach Daemon (http://www.talairach.org/daemon.html) where the Brodmann areas were identified from.

Group analysis and multiple-comparison correction

For all statistical parametric mapping analyses, random factor effects (RFXs) were used (random effect being the intercept of within-subject GLM fitting) and inferences were made at the group level to allow generalization to the population. For the group level inference, individual weighted β coefficient maps were fed into a one-sample *t* test that tested for the significance of group means of the factor of interest. The multiple comparison problem was dealt using cluster-extent thresholding within the Gaussian random field framework (Brett et al., 2003) implemented in SPM. Clusters were usually defined by a default primary voxel threshold of 0.001 (uncorrected). However, more stringent voxel-level thresholds were sometimes used because the statistical power in this study was very high and the conventional cluster-forming threshold of *p* uncorrected = 0.001 resulted in, in some occasions, clusters that were too extensive to be anatomically meaningful. In such cases, it has been suggested in the previous literature to use more stringent voxel-level threshold for making sensible inferences (Woo et al., 2014). Detailed threshold values used in this article for determining significant clusters as well as the significance statistics are reported in the result tables that we made accessible online (https://github.com/Aubrey-Lyu/data-analysis_Project_HCP_diffPCu/blob/main/group_results/Significance_tables.pdf). The FWE rate was controlled at the cluster level, and a threshold of *p* corrected $<$ 0.05 was used to determine the significance among clusters.

DCM specification

DCM is a generative model in a Bayesian framework for inferring hidden neuronal states from observed fMRI measurements. The causal influence estimated from the DCM is neurobiologically interpretable and describes the effect on the strength, or the rate of change, of synaptic connections among neuronal populations, as well as their context-sensitive modulation on external perturbation during tasks (Stephan et al., 2010). Using SPM12, our DCM model specified the endogenous connectivity between vPCu and dPCu to be bi-directional; and on top of that we modeled all possible configurations of how the task difficulty might influence the endogenous connectivity (Table 1). Since DCM is a generative model, it has to make assumptions about local neural populations in each region, and to this end, there are different kinds of neural mass models to choose from. In one-state models, each region is assumed to be composed of only single-state neurons, whose activity decays following a perturbation by exogenous input or incoming connections. In two-state models, each region is composed of both excitatory and inhibitory neural populations, the interaction of which can generate more complex dynamics (Marreiros et al., 2008). And stochastic models, compared with deterministic models, take into account neural noise for the local neural mass model (Daunizeau et al., 2012).

Table 1. The v/dPCu divisions resulted from the activated/deactivated clusters in the N-back and RP tasks

	Coordinate	dPCu Cluster size	*p*(cFWE-corr)
RP task	−4 −72 38	241	0.002
N-back task	8 −66 52	2175	0.000
	Coordinate	vPCu Cluster size	*p*(cFWE-corr)
RP task	−8 −60 18	216	0.005
N-back task	−8 −60 14	1547	0.000

The dPCu and vPCu were identified as the regions responsive to different cognitive load (the dPCu was activated while the vPCu was deactivated by an increased cognitive demand in difficult vs easy conditions). The N-back task provided a statistically stronger demonstration (larger significant clusters) of this, possibly because the task had more trials, i.e., bigger sample size (80 trials in the N-back, vs 27 in the RP task).

Our focus was on the directionality of connectivity at the regional level; therefore, we compared model structures representing all four combinations of how the two conditions (difficult vs easy) effected the mutual directional connectivity between v/dPCu. Based on that, both of the one-state, deterministic (the default) and the two-state, stochastic DCM class were used for modeling local neural dynamics.

DCM estimation

To determine the most likely model structure, we applied a fixed factor effect (FFX) Bayesian model selection (BMS) procedure to all 11 models estimated across all participants independently for the N-back and the RP task. The FFX model was used as opposed to a RFX, because we hypothesized the mechanism to be general across all subjects. Finally, the model with the highest model evidence was selected over others. Model evidence is the probability of obtaining the observed data given a particular model (Stephan et al., 2009).

Upon the selection of the best model structure, individuals' effective connectivity (EC) parameters were then correlated with their behavioral performance. To do so, linear regressions were conducted to probe the relationship between the RT and modulation of EC independently for the EC from dPCu to vPCu and the EC from vPCu to dPCu, with confounding covariates of age, sex and the mean activity of the vPCu and dPCu during tasks. The modulatory effect of task demand was estimated as the DCM parameters in the B matrix (Zeidman et al., 2019; https://www.fil.ion.ucl.ac.uk/spm/doc/spm12_manual.pdf). These parameters and RTs were logarithmic transformed to be more normally distributed.

Results

The DMN during tasks: a meta-analytic perspective

We first ascertained that the posteromedial DMN is indeed involved during goal-directed tasks, as findings regarding DMN's involvement during tasks are still disputed (Fransson, 2006). We conducted a meta-analysis with the latest *NeuroSynth* database, using a text-based filter ("attention* or execut*") to search for tasks that require either attention or executive processing or both (since the two cognitive processes are hardly separable in practice), which yielded 1219 fMRI studies. Using the forward-inference estimation, we found that a large portion of the DMN (1667 voxels) was associated with these tasks (Fig. 1*A*), with significant clusters ($Z > 4$) located at the PCu and AnG. In contrast, the reverse-inference estimation only revealed 68 voxels in DMN regions (Fig. 1*B*). We acknowledge that *NeuroSynth* meta-analyses do not differentiate between activation and deactivation but based on previous literature which has shown PCu

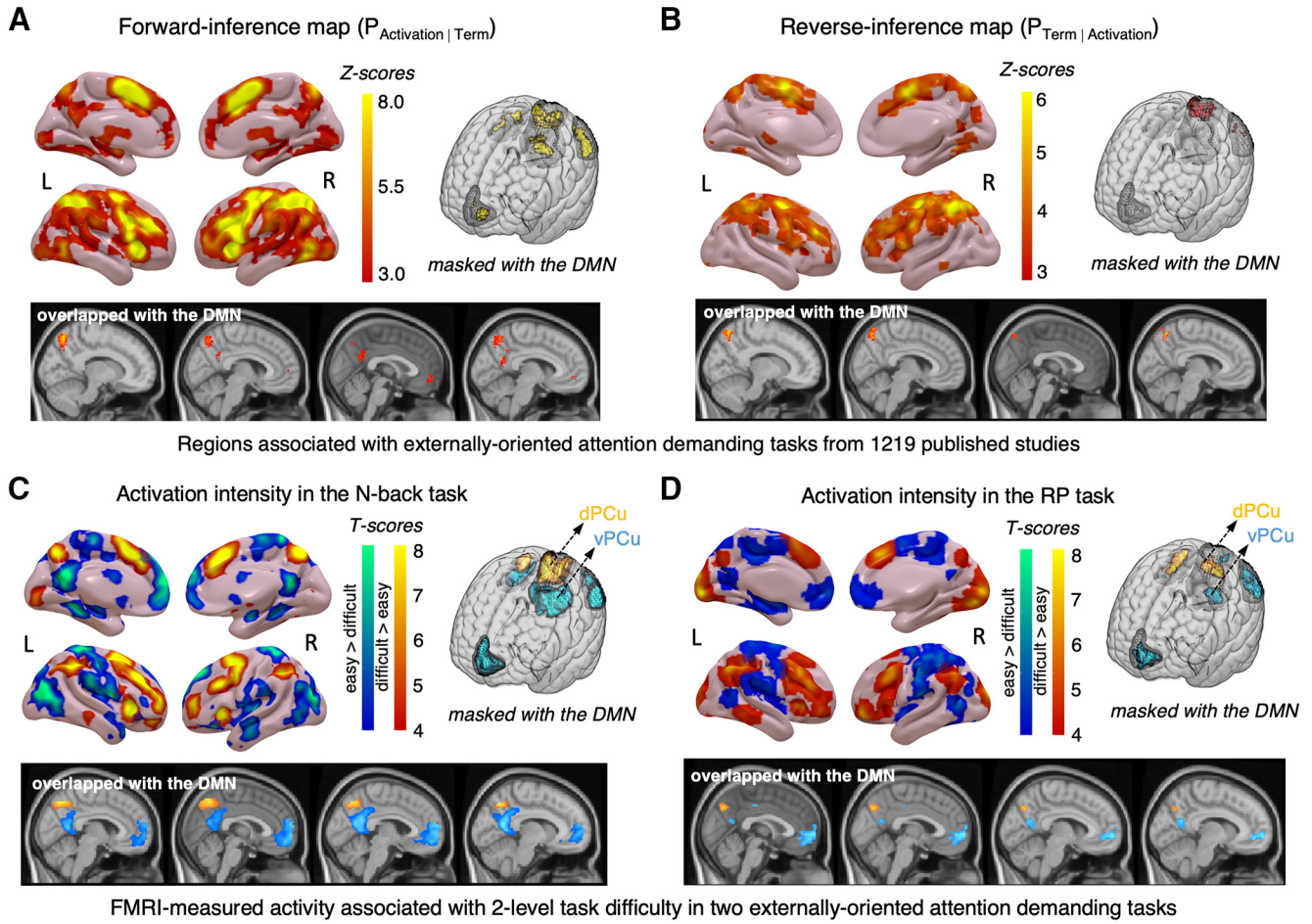

Figure 1. Meta-analysis and univariate analysis shows DMN engagement during the two tasks. ***A***, ***B***, *NeuroSynth* meta-analysis results, using "attention*" or "execut*" as keywords to search for goal-directed tasks that require attention and executive function. ***A***, Forward inference shows the DMN subregions that are active in the tasks. The forward inference map is produced by calculating the convergence of brain regions most consistently activated by certain cognitive processes. ***B***, Reverse inference shows that not many DMN regions are specifically associated with these tasks. The reverse inference map is calculated as the likelihood of a search term being used in a study given the presence of reported activation, and it reflects the brain activation specific to a certain cognitive process (Yarkoni et al., 2011). ***C***, ***D***, Activation of posterior DMN regions is associated with the N-back and RP task. Warm/cold regions in the brain heatmap indicate higher/lower activity in the difficult condition compared with the easy condition. For panels ***A***, ***B***, standardized Z scores and for panels ***C***, ***D***, T scores indicating activation strength are provided with color scales. For highlighting activation in relation to the DMN, 3D renderings of the DMN are shown in shaded gray, on which our activated regions are superimposed. This was constructed by superimposing the Z score maps (with the cutoff of 3) and T scores (of significant clusters with p(cFWE-corr) < 0.05), with the DMN atlas (as defined by the Conn network atlas). To highlight the posteromedial cortex clusters identified from the activation studies, we also provide sagittal views, where we only show the significant clusters within the DMN.

and AnG involvement in cognitive processing, we believe what we see here is that these tasks employ posterior DMN regions, yet their activation is so pervasive among all kinds of tasks that cannot be exclusively associated with the specified goal-directed tasks. The meta-analysis result indicates a domain-general role for posterior DMN areas which may serve cognitive demands by providing contextual information (Smith et al., 2021).

To capture more detailed statistical relationships of the internetwork interaction during task execution, we selected two fMRI paradigms (100 young healthy participants) from the HCP dataset. The tasks we chose were the N-back task and the RP task, which have attention-demanding, goal-directed features, and engage similar cognitive domains at two difficulty levels (N-back: 2-back > 0-back conditions, RP: RP > matching conditions). The two tasks afforded us the possibility of inferring the brain's response to varying cognitive demands regardless of the specific cognitive content (working memory or RP in this study), thus indicating that the statistical relationship we picked up may be generalizable to other tasks when high-level cognitive effort is involved. As a sanity check for both tasks, the accuracy rate (N-back task: $t = 2.44$, $p = 0.02$; RP task: $t = 8.80$, $p = 0.00$) was significantly higher in the easy than difficult conditions, and RTs were significantly shorter (N-back task: $t = 10.58$, $p = 0.00$; RP task: $t = 10.02$, $p = 0.00$), suggesting that the cognitive load in difficult conditions was indeed higher than in easy conditions. To avoid task-irrelevant cognitive confounds, we only included trials with correct responses for further statistical analyses.

The activation result showed that most of the task-induced activations corresponding to more difficult conditions were located in cognitive control regions, while the deactivated areas were found in the DMN (Fig. 1*C*,*D*). However, significant activations were also found in the AnG and the PCu, which are assigned to the DMN by the two brain atlases (from two independent studies) that we adopted in this study [see Materials and Methods: Selection of regions of interest (ROIs) and Anatomical labels and ICN identification based on significant clusters]. As a result, for both tasks, the PCu was consistently differentiated into dorsal and ventral parts (dPCu, vPCu; Table 1; Fig. 2), which were, respectively, more active during higher and lower cognitive demand conditions.

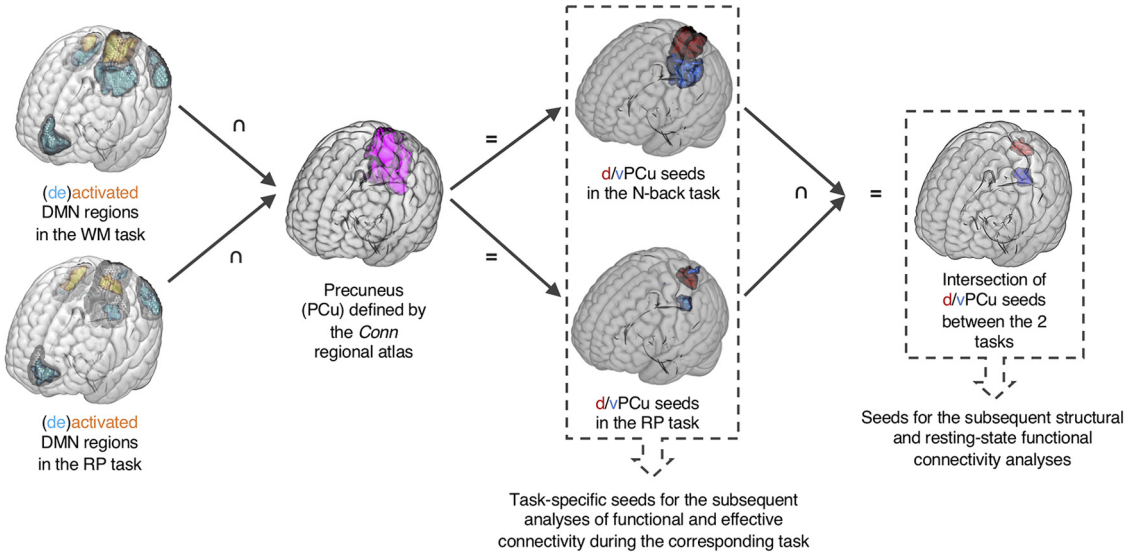

Figure 2. Seed derivation for the connectivity analyses. Task-specific seeds for FC and EC during tasks were derived by overlapping activation maps from either the N-back or RP task, and the DMN and PCu masks from the Conn network and regional atlases. Analysis for each task was conducted independently. For task-independent structural FC and rsFC, the PCu seeds (d/vPCu) were defined as the spatial intersection of the activated or deactivated clusters in both tasks, the DMN and the PCu masks.

Differential connectivity between v/dPCu and ICNs

To explore further the differential network associations of the dorsal and ventral aspects of the PCu, we next focused on the d/vPCu's connectivity, including structural, resting-state, task-state and task-related connectivity. As a sanity check, before we contrasted the whole-brain maps of the d/vPCu's SC, we compared the global average strength of the d/vPCu whole-brain SC, which was shown to not be significantly different by a paired t test ($t = 0.90$, $p = 0.37$). Hence, we could interpret the v/dPCu SC contrasts as reflecting the difference of the regional connectivity densities between the v/dPCu. In addition, we also measured the baseline rsFC to show that for our dataset both of the v/dPCu's FC is mainly located within the DMN during rest (Additional information regarding this result can be found in: https://github.com/Aubrey-Lyu/data-analysis_Project_HCP_diffPCu/blob/main/research_paper___Precuneus_SI.pdf (Figure 1. Resting-state seed-based FC of the d/vPCU. Figure 2. Spatial localization of the dPCu (a) and vPCu (b) with respect to the canonical DMN.)), which conforms to the broader definition of the DMN (Raichle, 2015).

By contrasting between the connectivity of the two seeds, we demonstrated that there are regional differences both in the SC and rsFC between the vPCu and dPCu, which follow the pattern of internally and externally oriented cognitive function, according to our task-based coactivation network atlas. Specifically, by comparing the vPCu and dPCu's whole-brain SC, we found that the vPCu is more connected with the vmPFC, ACC and hippocampus, which are often implicated in value encoding, emotion, interoception and episodic memory (Pessoa, 2008; Euston et al., 2012; Chudasama et al., 2013; Gu et al., 2013), while the dPCu is more connected with regions in cognitive control networks that are associated with executive, attentional control and goal-directed behavior (Fig. 3*A*). We also found similar differentiation in rsFC of the d/vPCu (Fig. 3*B*).

To establish whether the differential network associations between the d/vPCu also hold for a task-engaged brain, we next compared the d/vPCu's FC patterns during tasks by computing the so-called endogenous tsFC, i.e., the correlation of timeseries throughout the course of the two tasks, after regressing out the stimuli-evoked activation. Despite being regressed out, there might be residuals from the activation effect. However, we are interested in the difference between the d/vPCu connectivity: since the activation effect is modeled the same way for both seeds; should residuals exist, they would be contrasted off by comparing between the d/vPCu's tsFC (see more details in Materials and Methods: Task-state seed-based FC of v/dPCu). Again, we found similar patterns of differential connectivity between the v/dPCu with the IoN and the EoN (Fig. 3*C*). Notably, unlike the SC and rsFC results, where the visual network was more strongly connected with the vPCu compared with dPCu, the tsFC between the dPCu and visual networks were stronger instead. As both of the tasks we used were based on visual information, the tsFC contrast result suggested that the dPCu was more engaged in integrating incoming information from the external world during tasks.

Cognitive demands modulate the effective coupling between the d/vPCu and IoN/EoN

The connectivity profiles of the d/vPCu as established so far suggest that the PCu overall has the structural framework necessary to serve as a platform connecting internal and externally related information. To confirm that this is cognitively relevant, we investigated whether d/vPCu connectivity during tasks is modulated by cognitive load and whether this modulatory effect is correlated with task performance. We therefore investigated the PPI effect and its relationship with the participants' behavioral performance.

PPI is a GLM with an interaction effect that allows us to investigate differences in FC between two experimental conditions (see Materials and Methods, PPIs). We call such FC that tracks variable cognitive demand trFC. Using PPI, we found that as cognitive demand increased, trFC increased between the vPCu and IoN and between the dPCu and EoN. However, when the cognitive demand was low the trFC association was reversed (Fig. 4). In other words, the dPCu was more connected to visual and motor networks in difficult (vs easy) conditions, and more connected to DMN regions in easy (vs difficult) conditions. On the contrary, the vPCu was more connected to the rest of the DMN and interoceptive regions in difficult (vs easy) conditions, and more connected with visual and primary sensory networks in easy (vs difficult) conditions (Fig. 4*C*).

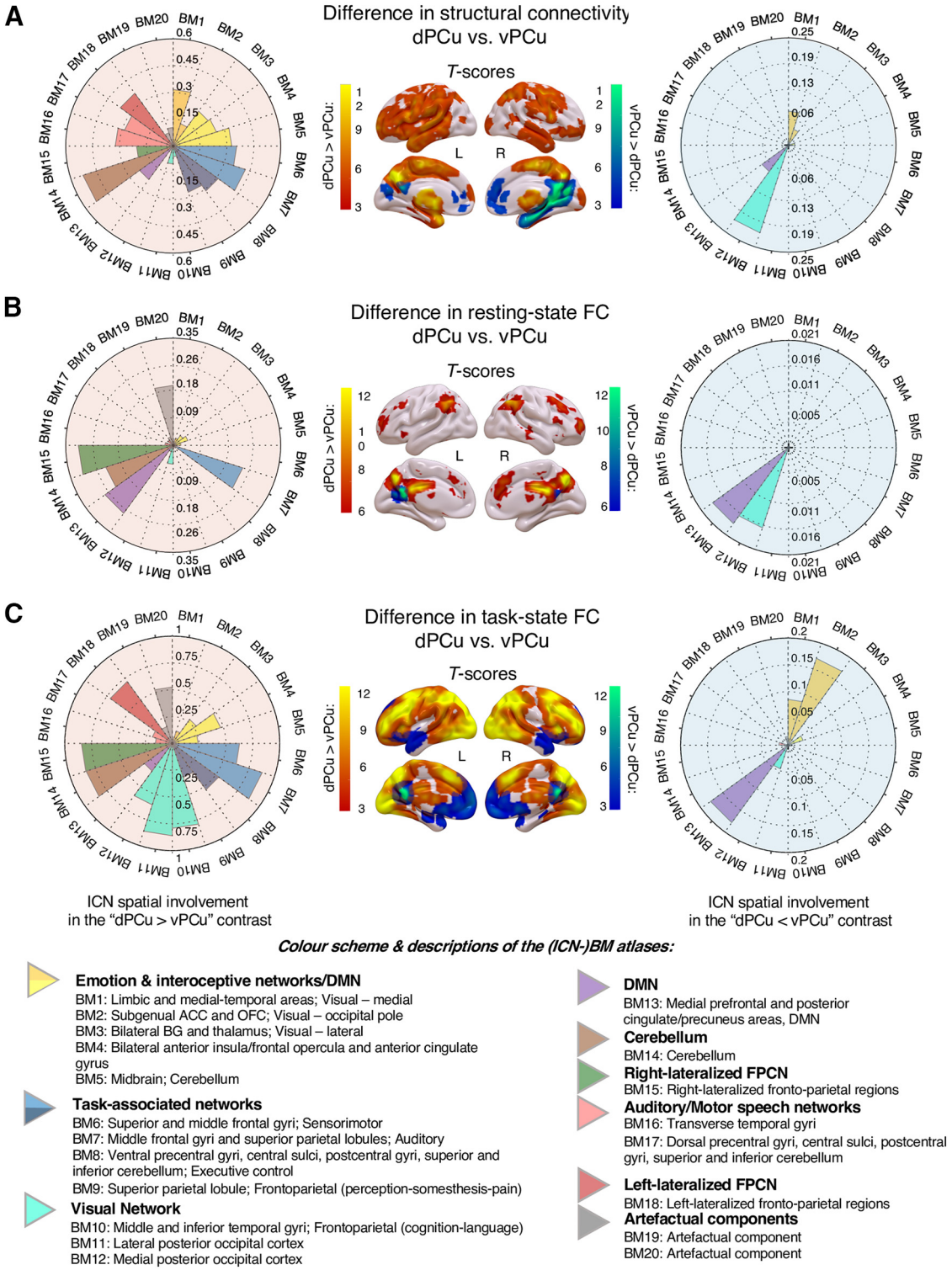

Figure 3. Whole-brain contrasts of the connectivity between dPCu and vPCu. SC is in ***A***, rsFC in ***B***, and tsFC in ***C***. tsFC was calculated as a partial correlation, controlling for the effect of event-related BOLD signals (i.e., disregarding the apparent correlation caused by stimulus-driven activity). T scores for the statistical effect of the connectivity difference are mapped out on the 3D brain reconstructions. Hot colors represent areas that demonstrate stronger connectivity with the dPCu than with the vPCu, and vice versa for the cold colors. Circular wedge plots to the left and right are a representation of ICN spatial involvement, i.e., show voxel overlap between canonical ICNs and the connectivity results. The canonical ICNs are defined by the ICN-BM atlases from the *ICN_atlas* toolbox (Kozák et al., 2017). Cognitive domains and descriptions of the ICN-BM atlases for the ICNs are also provided. The same color scheme for the (ICN-)BM atlases was used throughout the article.

In order to rule out the possibility that the reversed modulation of the v/dPCu's FC might be because of a spurious statistical relationship created by the anticorrelation between the two, we conducted a follow-up investigation and found the timeseries of vPCu and dPCu were positively correlated throughout the experiment (Pearson-correlation coefficient is 0.25 for the N-back task and 0.27 for the RP task). Therefore, the reversed modulation of the seed-network associations cannot be explained by

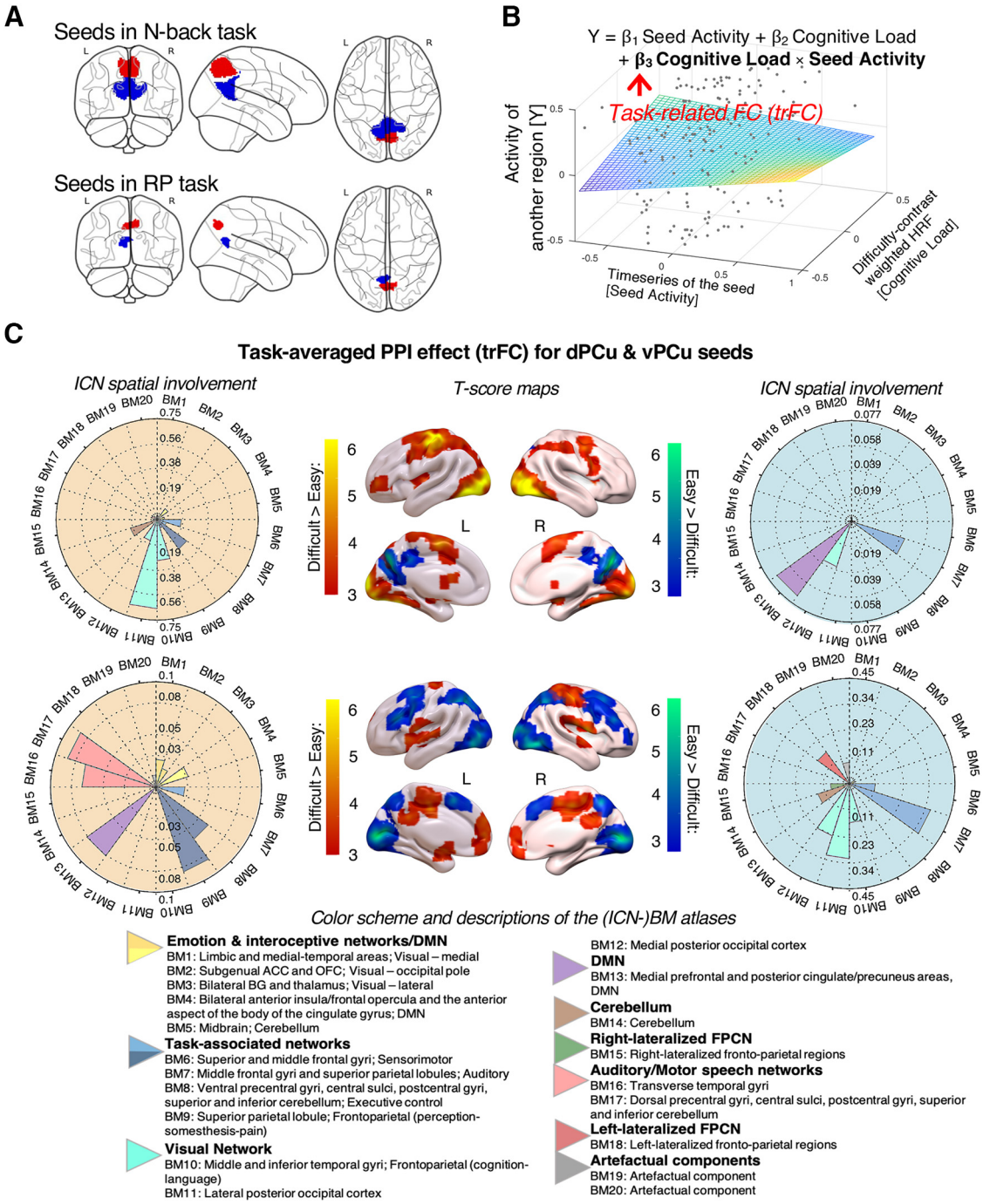

Figure 4. PPI analyses for the two tasks revealed an inverse pattern of the trFC of the two seeds (dPCu and vPCu), which is common to both tasks. ***A***, Functional seeds of the dPCu (red) and vPCu (blue) in the N-back and the RP task, visualized from posterior (left), lateral (middle), and superior (right) perspectives. The two clusters (dPCu and vPCu) were shown to be significant activated and deactivated, respectively, by increased task demand in the N-back and RP tasks, according to the previous activation studies. ***B***, Illustration of the PPI statistical model, generated from data of a randomly selected participant. As shown, the relationship between the seed region and the rest of the brain is dependent on the cognitive demands. ***C***, The whole-brain T score maps showed the PPI effect (trFC) for the reversed contrasts: difficult > easy and easy > difficult conditions, for the two seeds: d/vPCu, averaged across the N-back and RP tasks. Warm colors on the brain maps indicate the regions whose FC with the seed is increased on an increased cognitive demand (difficult > easy), while cold colors indicate the regions whose FC with the seed is decreased on an increased cognitive demand (easy > difficult). The circular wedge plots besides the brain heatmap indicate the ICN spatial involvement of the significant regions in the corresponding contrast, i.e., voxel overlap between canonical ICNs and the connectivity results. The canonical ICNs are defined by the ICN-BM atlases from the ICN atlas toolbox (Kozák et al., 2017). Cognitive domains and descriptions of the ICN-BM atlases for the ICNs are provided below.

the anticorrelation between the seeds, but rather reflected an opposite direction of modulatory effect.

Further, we found that the positive trFC between vPCu and IoN, and between dPCu and EoN, are negatively correlated with the increased RT that participants needed in the difficult (vs easy) condition. Specifically, the trFC between the dPCu and FPCN regions (including inferior frontal gyrus, medial frontal gyrus and superior temporal gyrus) was significant in this analysis as was the trFC between the vPCu and DMN regions (including AnG, PCu, and precentral gyrus; Fig. 5). It is noteworthy that

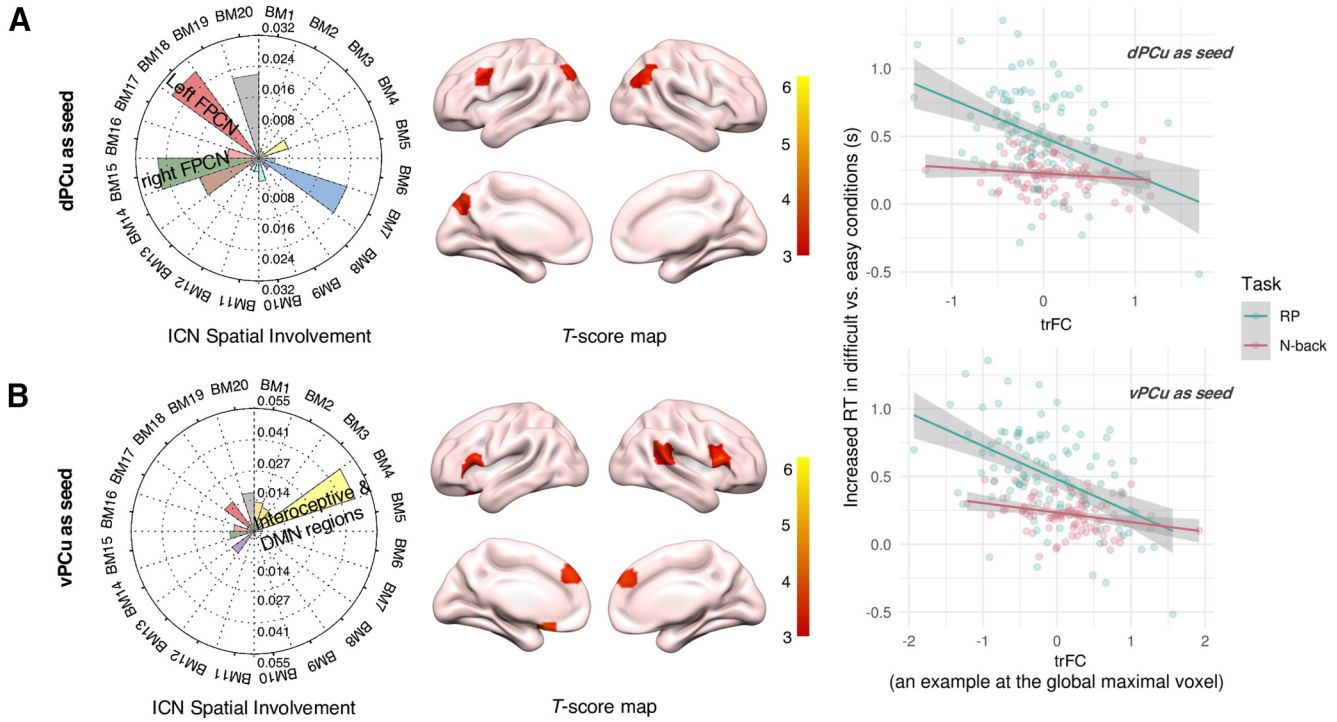

Figure 5. Task modulation of the d/vPCu's FC (i.e., trFC) from the PPI analysis is correlated with RT of correct responses. (A) and (B) respectively show that the trFC between dPCu and the bilateral frontoparietal regions, and the trFC between the vPCu and the regions in the "interoceptive" network, are correlated with RT. ICN-BM involvement of the significant regions is demonstrated using the ICN_atlas toolbox (also see Fig. 3). Scatter plots to the right depict the linear relationships between trFC and (relative) RT for the peak voxels.

Config. \ Model	1	2	3	4	5	6	7	8	9	10	11
endogenous EC	V↔D	V↔D	V↔D	V↔D	V↔D	V↔D	V↔D	V↔D	V↔D	V↔D	V↔D
modulated EC (difficult)	V→D	D→V	V→D	D→V	V↔D	V→D	D→V	V→D	D→V	V→D	D→V
modulated EC (easy)	V→D	D→V	D→V	V→D	V↔D	V→D	D→V	D→V	V→D	none	none
local neural model 1 = one-state & deterministic 2 = two-state & stochastic	1	1	1	1	2	2	2	2	2	2	2
posterior probability in N-back	0.00	0.64	0.35	0.00	0.00	0.00	0.00	0.00	0.00	0.00	0.00
posterior probability in RP	0.00	0.00	0.99	0.00	0.00	0.00	0.00	0.00	0.00	0.00	0.00
(relative) model evidence in N-back	0	15.51	14.93	8.27							
(relative) model evidence in RP	23.48	29.07	55.09	0							

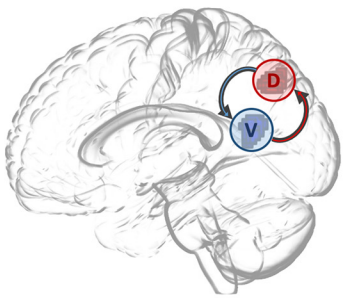

Figure 6. Model comparison result suggesting that the causal influence from the dPCu to vPCu is modulated in easier conditions and then swapped from the vPCu to dPCu in more difficult conditions. The first four rows/aspects of the model structure specified 11 DCM models. The first four DCMs that adopted "one-state," "deterministic" neural mass model won over the "two-state," "stochastic" ones, according to the posterior probability at the group level (assuming an FFX). Among the "one-state," "deterministic" DCMs, the third model wins over others with consistently higher posterior probability and higher exceedance of model evidence.

trFC predicted task performance while the contrast-based activation did not.

The causal influence from dPCu →vPCu and from vPCu →dPCu was differentially modulated on low and high cognitive demand

Our findings so far suggest that the v/dPCu are, respectively, focused on internal and externally relevant information processing. To obtain further evidence that the PCu is the brain region where these two types of information get integrated, we explored the directionality of information flow between the vPCu and dPCu and its modulation by task demands.

To achieve this, we adopted the DCM framework which infers evidence for causal connectivity between regions on external perturbation during a task (Stephan et al., 2010). According to our hypothesis, we specified 11 possible model structures, based on how the task difficulty might modulate causal connectivity between the vPCu and dPCu (Fig. 6). All of the model structures have a recurrent structure of the endogenous EC between dPCu and vPCu (i.e., the A matrix in the DCM terminology), while the model comparisons were focused on the exogenous EC in the B matrix, which specifies the modulation (namely, the rate of change) of the EC because of experimental conditions (Zeidman et al., 2019).

Bayesian model comparisons among the 11 models showed that, for the micro-circuit neural model embedded in the DCM, the bi-linear, one-state and deterministic model class was better for fitting our data than the nonlinear, two-state and stochastic

Table 2. Modulation of EC in different conditions during tasks

	RP ($n = 98$)		N-back ($n = 96$)	
Condition	Difficult	Easy	Difficult	Easy
EC direction	vPCu →dPCu	dPCu →vPCu	vPCu →dPCu	dPCu →vPCu
B_E	0.008 ± 0.060	0.011 ± 0.054	0.001 ± 0.002	0.002 ± 0.003

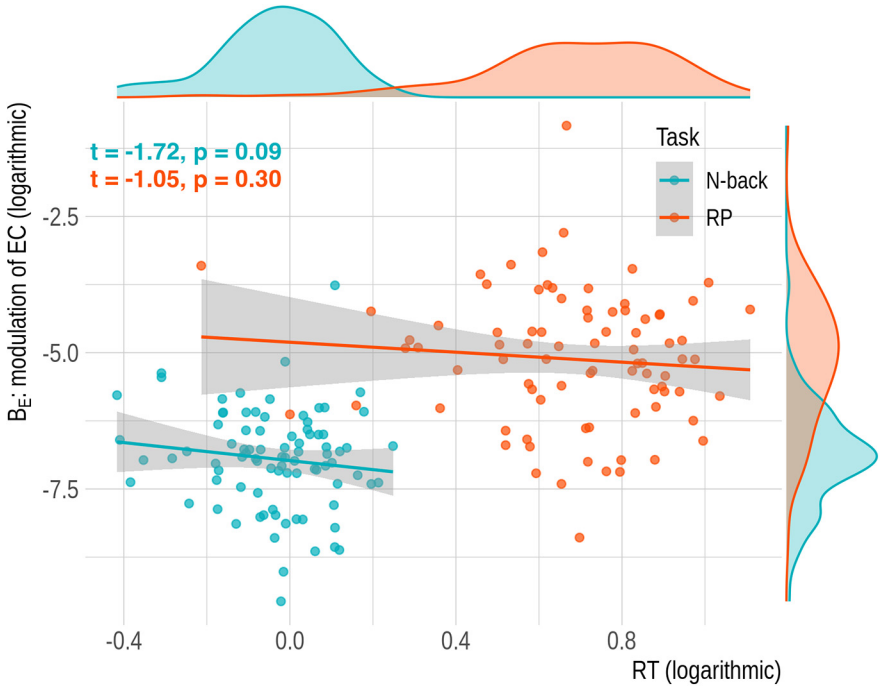

Figure 7. Behavioral relevance of the (positive) modulation effect on the EC (vPCu →dPCu) caused by higher cognitive demand during the N-back and RP tasks. Scatter plot depicts the relationship between the RT and B_E (the modulation of EC) in the logarithmic scale. Distributions of the data have also been presented at the scatter plot's margins.

one (Marreiros et al., 2008), with an exceedance of log-evidence (an indication of how good a model is by weighing the goodness of data fitting against the model complexity) $>1 \times 10^{16}$ in the N-back task and $>5 \times 10^{16}$ in the RP task (Fig. 6). By comparing the possible ways of how task difficulty modulated the directed information flow we established two models which had higher model evidence than the others: (1) the "exchange" model, which specifies an EC modulation of dPCu →vPCu in the easy condition and vPCu →dPCu in the difficult condition; (2) the "forward" model, which specified the EC of dPCu →vPCu to be modulated in both difficult and easy conditions. In the RP task, the exchange model was identified as the single winning model by the BMS (Fig. 6). Although in the N-back task the forward model had higher posterior probability than the exchange model by 0.3, the magnitude of its model evidence did not allow us to draw a safe conclusion of favoring it over the other model.

The behavioral relevance of the EC from vPCu to dPCu

In order to show that the reciprocal EC between d/vPCu was behaviorally relevant, we did further statistical testing to examine the relationship between the modulation of EC and the RT for correct responses. Statistical testing was focused on the parameters in the B matrix of the exchange model. The model structure of the exchange model suggests the EC from dPCu to vPCu to be upregulated by the cognitive requirement in the easy condition and the EC from vPCu to dPCu to be upregulated by the cognitive demand in the difficult condition. The extrinsic EC values in the B matrix parameters (B_E) indicate the modulation effects on the above EC that are caused by the external cognitive bearing in each condition (Zeidman et al., 2019).

The B_E of vPCu →dPCu in difficult conditions was 0.005 (SD = 0.043, $p = 0.000$), and the B_E of dPCu →vPCu in easy conditions was 0.07 (SD = 0.039, $p = 0.000$), both significantly higher than zero as established by one-sample Wilcoxon tests. The B_E of vPCu →dPCu was significantly larger in the RP task than in the N-back task ($t = 3.277$, $p = 0.001$), while the EC of dPCu →vPCu was not different between the RP and N-back task (Table 2). The correlation between the RT and the positive B_E was examined for the modulation effect on the EC (vPCu →dPCu) in the difficult condition. The regression line for these two variables has a negative slope, suggesting that the more the EC was strengthened on the cognitive load, the quicker the RT became. Despite this trend, the test was not significant ($t = -1.72$, $p = 0.09$ for the N-back, and $t = -1.05$, $p = 0.30$ for the RP task; see Fig. 7).

Additional information

Additional information regarding experimental descriptions for the task-related fMRI data, seed-based FC of the dPCu and vPCu during rest and tasks, the correspondence between brain region and network atlases, and several validations of ICN involvements in the d/vPCu's trFC from the PPI analysis can be found in: https://github.com/Aubrey-Lyu/data-analysis_Project_HCP_diffPCu/blob/main/research_paper___Precuneus_SI.pdf.

Discussion

The present study investigated the functional differentiation of the posteromedial DMN and proposed a role for the PCu in mediating external and internal information binding. We showed that the PCu has differential connectivity with the rest of the DMN and cognitive control networks. These are not an epiphenomenon of structural FC or rsFC, instead they track cognitive demands in a working memory and a high-order RP task. In addition, we found evidence for directed interactions from dPCu to vPCu during easier cognitive conditions and from vPCu to dPCu during more difficult conditions. Although the tasks we chose were targeting specific cognitive domains, i.e., working memory and RP, we focused on the common pattern of the whole-brain connectivity, not only across the two tasks, but also considered SC and rsFC. Instead of relying on the common practice of forward inference, by which we associate brain regions to certain function based on task features; here we relied on reverse inference (Hutzler, 2014), i.e., to infer implicit cognitive processing during a task based on the brain regions involved, whose function has been well characterized in the previous literature. Reverse inference is considered appropriate here, because our

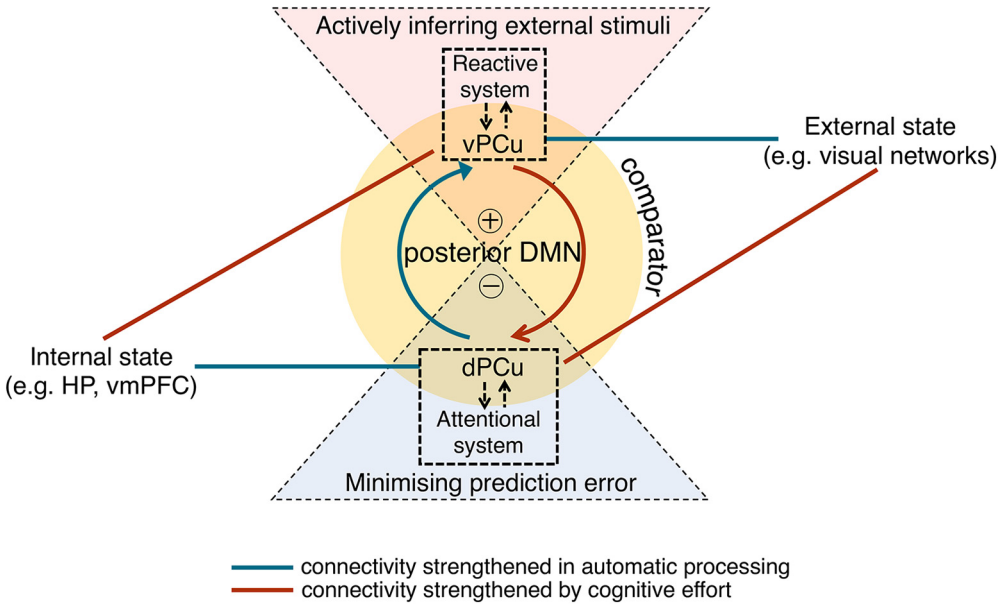

Figure 8. A conceptual predictive model centering at the posterior medial DMN. The posterior medial DMN behaves like a predictive system, with its dorsal part associated with an attentional system (comprising FPCN regions such as the IPS and middle and lateral frontal cortices) and its ventral part associate with a reactive system (comprising regions such as anterior insula; Tops et al., 2014). The connectivity from each module is derived from our studies, with the red lines indicating stronger connectivity in difficult conditions, and blue lines indicating stronger connectivity in easy conditions. The (directed) connectivity pattern from our result suggests that external and internal information is exchanged by the reciprocal loop between the vPCu and dPCu. This exchange of information might support the predictive coding theory which emphasizes that external information is always inferred (rather than simply being represented from a bottom-up direction) based on an internal belief of the world (prediction).

experimental questions concern broad cognitive domains, i.e., internally or externally oriented cognition, and the DMN and the FPCN/visual network have been well characterized in the literature as, respectively, internally and externally oriented. Taking this into consideration, our results highlight a causal interaction between the different information processing streams of the d/vPCu for binding internal (e.g., self-related or high-level stored information) and external (e.g., incoming environmental stimuli) information.

Although previous work also hinted at the different roles in the ventral and dorsal parts of the PCu, this is the first systematic demonstration that the v/dPCu are, respectively, more closely connected to IoN and EoN. A previous rsFC study showed that the vPCu is functionally closer to the DMN, while the dPCu is more coupled with the superior occipital lobe and cognitive control regions such as the superior parietal lobules (SPLs; Zhang and Li, 2012). A SC study also showed that from dorsal to ventral parts of the PCu, there is a spectrum of increasing connectivity with DMN regions (such as hippocampus and mPFC) and decreasing connectivity with sensorimotor, visual networks, thalamus and executive regions (such as SPL and prefrontal and premotor areas; Cunningham et al., 2017).

In a previous task-based study, Leech and colleagues using a dual N-back experiment found a functional differentiation between the (deactivated) dorsal PCC and the (activated) ventral PCC (Leech et al., 2011). The dorsal PCC in their study is close to what we call vPCu in this study. This region (BA 31) lies in the borders between BA 7 (PCu) and BA 23 (PCC) and has been considered to be part of the PCu or PCC by different authors (Cavanna and Trimble, 2006). Leech and colleagues identified distinct FC patterns of ventral PCC and dorsal PCC, the former not only decreasing its positive FC with the DMN but also reducing the negative FC with cognitive control networks (thus being less integrated with the whole brain in general); on the other hand, they found the dorsal PCC increased its connectivity with both the DMN and cognitive control networks, in the difficult versus easy contrast. Noticeably, we did not find any significant negative FC for our PCu seeds. Non-neuronal noise is unlikely the reason for our lack of anticorrelation here, because we have taken rigorous measures to alleviate non-neuronal noise sources, over and above the data-driven denoising utilised in the HCP preprocessing pipeline. Furthermore, there have been studies casting doubts on the nature of the anticorrelation between the DMN and task-positive networks, suggesting that the anticorrelation diminishes when global signal regression is avoided or high-frequency signals are considered (Caballero-Gaudes and Reynolds, 2017; Craig et al., 2018).

A recent study probing the DMN's role in auto-pilot behavior suggested that via the connectivity between PCC/PCu and middle temporal lobe, the brain gains access to stored information and utilises learnt rules to complete the task at hand (Vatansever et al., 2017). Here, by using two levels of difficulty, we also found that when more cognitive effort was needed, stored information was employed. This manifested in the form of increasing connectivity between the vPCu and other parts of the DMN and elevated causal influence from the vPCu to dPCu; meanwhile, the dPCu connected more with attentional systems dealing with increased difficulty and lack of readily available answers.

We propose to interpret our series of findings through the lens of the predictive coding theory (Friston, 2010; Tops et al., 2014; Fig. 8). Accordingly, externally driven and internally driven information are exchanged in the PCu and this process is mediated by a "causal loop" between the PCu's dorsal and ventral subdivisions. By binding internal priors encoded in high-level cortex (gradually shaped from previous experience) and external representations from sensory cortices, the brain acts as Bayesian machine to interpret ambiguous and quickly shifting environmental cues.

The functional differentiation within the PCu may just be an iceberg tip in terms of DMN characteristics. It has been

suggested in the previous literature that the DMN is a "transmodal" region which encompasses several networks (Braga et al., 2013; Braga and Buckner, 2017; Kernbach et al., 2018). In addition, the subregions of the DMN can take different roles in different tasks. For example, the AnG is for attentional control and semantic comprehension (Seghier, 2013; Lambon-Ralph et al., 2017; Lyu et al., 2019), ACC for value-based perception and error detection (Fleck et al., 2006; Chudasama et al., 2013; Monosov, 2017) and hippocampus for memory encoding (Bird and Burgess, 2008) etc. However, the PCu's function seems to have an all-encompassing nature since it is activated under all kinds of cognitive demand where other parts of DMN are employed (Laird et al., 2009). Indeed, graph theoretic analyses on the human brain connectome have suggested that the PCu is the central hub of brain connectivity (Tomasi and Volkow, 2011; van den Heuvel and Sporns, 2013). The PCu, besides the DMN, has also been found to be most closely connected to the thalamus (Cunningham et al., 2017). At this brain connectivity hub, information from all sources converges, endowing a narrative construction of reality: it have also been shown that during movie watching the temporal pattern of the PCu's activity, compared with other brain regions, can track event boundaries of changing scenes in the most abstract level (Baldassano et al., 2017). Based on previous work and our current study, we believe the PCu is central for linking the function of the DMN subdivisions, thus playing a key role in integrating the brain's information flow from all sources.

Although the PCu was our focus in this study, it is not the only DMN subregion that demonstrates a functional fragmentation. We also observed a similar functional differentiation in the AnG's activation pattern, but only in the N-back task. Evidence also comes from previous studies which have discussed the activation patterns of the DMN subregions, such as the mPFC (Bzdok et al., 2013; Kuzmanovic et al., 2018), the IPL (Igelström and Graziano, 2017), the PCC (Leech et al., 2011), and the PCu (Cavanna and Trimble, 2006). Taken together, the evidence suggests that these regions may be functionally subdivided according to a ventral-dorsal (or anterior-posterior) topographical structure. We therefore postulate that the DMN might comprise ventral/anterior and dorsal/posterior subdivisions that act as interfaces between self (internal)-related and environmental-related processing. Our study is agnostic about possible functional subdivisions of other DMN regions besides the PCu, but future studies should continue the exploration of the functional differentiation between and within the DMN subregions. The DMN has been postulated to be at the highest level of information processing in the brain (Margulies et al., 2016) and has the highest number of optimal inter-network connections in the brain (Pappas et al., 2020), along with our findings presented here, we propose that this topological division of internal and external related functions may be a necessary consequence of developmental optimization of information processing. By continuing this line of investigation, we might gain important insights into the brain's functional organization.

References

Allen M, Friston KJ (2018) From cognitivism to autopoiesis: towards a computational framework for the embodied mind. Synthese 195:2459–2482.

Baldassano C, Chen J, Zadbood A, Pillow JW, Hasson U, Norman KA (2017) Discovering event structure in continuous narrative perception and memory. Neuron 95:709–721.e5.

Barch DM, Burgess GC, Harms MP, Petersen SE, Schlaggar BL, Corbetta M, Glasser MF, Curtiss S, Dixit S, Feldt C, Nolan D, Bryant E, Hartley T, Footer O, Bjork JM, Poldrack R, Smith S, Johansen-Berg H, Snyder AZ, Van Essen DC, et al. (2013) Function in the human connectome: task-fMRI and individual differences in behavior. Neuroimage 80:169–189.

Barrett LF, Simmons WK (2015) Interoceptive predictions in the brain. Nat Rev Neurosci 16:419–429.

Brett M, Penny W, Kiebel S (2003) An introduction to random field theory. Human Brain Function, pp 867–879. Academic Press.

Bird CM, Burgess N (2008) The hippocampus and memory: insights from spatial processing. Nat Rev Neurosci 9:182–194.

Braga RM, Buckner RL (2017) Parallel interdigitated distributed networks within the individual estimated by intrinsic functional connectivity. Neuron 95:457–471.e5.

Braga RM, Sharp DJ, Leeson C, Wise RJS, Leech R (2013) Echoes of the brain within default mode, association, and heteromodal cortices. J Neurosci 33:14031–14039.

Bressler SL, Menon V (2010) Large-scale brain networks in cognition: emerging methods and principles. Trends Cogn Sci 14:277–290.

Bzdok D, Langner R, Schilbach L, Engemann DA, Laird AR, Fox PT, Eickhoff SB (2013) Segregation of the human medial prefrontal cortex in social cognition. Front Hum Neurosci 7:232.

Caballero-Gaudes C, Reynolds RC (2017) Methods for cleaning the BOLD fMRI signal. Neuroimage 154:128–149.

Cavanna AE, Trimble MR (2006) The precuneus: a review of its functional anatomy and behavioural correlates. Brain 129:564–583.

Chai XJ, Castañón AN, Ongür D, Whitfield-Gabrieli S (2012) Anticorrelations in resting state networks without global signal regression. Neuroimage 59:1420–1428.

Chudasama Y, Daniels TE, Gorrin DP, Rhodes SE, Rudebeck PH, Murray EA (2013) The role of the anterior cingulate cortex in choices based on reward value and reward contingency. Cereb Cortex 23:2884–2898.

Cole MW, Bassett DS, Power JD, Braver TS, Petersen SE (2014) Intrinsic and task-evoked network architectures of the human brain. Neuron 83:238–251.

Cole MW, Ito T, Bassett DS, Schultz DH (2016) Activity flow over resting-state networks shapes cognitive task activations. Nat Neurosci 19:1718–1726.

Craig MM, Manktelow AE, Sahakian BJ, Menon DK, Stamatakis EA (2018) Spectral diversity in default mode network connectivity reflects behavioral state. J Cogn Neurosci 30:526–539.

Cunningham SI, Tomasi D, Volkow ND (2017) Structural and functional connectivity of the precuneus and thalamus to the default mode network. Hum Brain Mapp 38:938–956.

Daunizeau J, Stephan K, Friston K (2012) Stochastic dynamic causal modelling of fMRI data: should we care about neural noise? Neuroimage 62:464–481.

de Pasquale F, Della Penna S, Snyder AZ, Marzetti L, Pizzella V, Romani GL, Corbetta M (2012) A cortical core for dynamic integration of functional networks in the resting human brain. Neuron 74:753–764.

Demertzi A, Soddu A, Laureys S (2013) Consciousness supporting networks. Curr Opin Neurobiol 23:239–244.

Elton A, Gao W (2015) Task-positive functional connectivity of the default mode network transcends task domain. J Cogn Neurosci 27:2369–2381.

Euston DR, Gruber AJ, McNaughton BL (2012) The role of medial prefrontal cortex in memory and decision making. Neuron 76:1057–1070.

Fleck MS, Daselaar SM, Dobbins IG, Cabeza R (2006) Role of prefrontal and anterior cingulate regions in decision-making processes shared by memory and nonmemory tasks. Cereb Cortex 16:1623–1630.

Fletcher PC, Happé F, Frith U, Baker SC, Dolan RJ, Frackowiak RS, Frith CD (1995) Other minds in the brain: a functional imaging study of "theory of mind" in story comprehension. Cognition 57:109–128.

Fox MD, Snyder AZ, Vincent JL, Corbetta M, Essen DCV, Raichle ME (2005) The human brain is intrinsically organized into dynamic, anticorrelated functional networks. Proc Natl Acad Sci USA 102:9673–9678.

Fransson P (2006) How default is the default mode of brain function?: further evidence from intrinsic BOLD signal fluctuations. Neuropsychologia 44:2836–2845.

Friston K (2010) The free-energy principle: a unified brain theory? Nat Rev Neurosci 11:127–138.

Friston K (2012) The history of the future of the Bayesian brain. Neuroimage 62:1230–1233.

Friston K, Kiebel S (2009) Predictive coding under the free-energy principle. Philos Trans R Soc Lond B Biol Sci 364:1211–1221.

Glasser MF, Sotiropoulos SN, Wilson JA, Coalson TS, Fischl B, Andersson JL, Xu J, Jbabdi S, Webster M, Polimeni JR, Van Essen DC, Jenkinson M; WU-Minn HCP Consortium (2013) The minimal preprocessing pipelines for the human connectome project. Neuroimage 80:105–124.

Gu X, Hof PR, Friston KJ, Fan J (2013) Anterior insular cortex and emotional awareness. J Comp Neurol 521:3371–3388.

Hutzler F (2014) Reverse inference is not a fallacy per se: cognitive processes can be inferred from functional imaging data. Neuroimage 84:1061–1069.

Igelström KM, Graziano MSA (2017) The inferior parietal lobule and temporoparietal junction: a network perspective. Neuropsychologia 105:70–83.

Ito T, Kulkarni KR, Schultz DH, Mill RD, Chen RH, Solomyak LI, Cole MW (2017) Cognitive task information is transferred between brain regions via resting-state network topology. Nat Commun 8:1027.

Kernbach JM, Yeo BTT, Smallwood J, Margulies DS, de Schotten MT, Walter H, Sabuncu MR, Holmes AJ, Gramfort A, Varoquaux G, Thirion B, Bzdok D (2018) Subspecialization within default mode nodes characterized in 10,000 UK Biobank participants. Proc Natl Acad Sci USA 115:12295–12300.

Kozák LR, van Graan LA, Chaudhary UJ, Szabó ÁG, Lemieux L (2017) ICN_Atlas: automated description and quantification of functional MRI activation patterns in the framework of intrinsic connectivity networks. Neuroimage 163:319–341.

Kuzmanovic B, Rigoux L, Tittgemeyer M (2018) Influence of vmPFC on dmPFC predicts valence-guided belief formation. J Neurosci 38:7996–8010.

Laird AR, Eickhoff SB, Li K, Robin DA, Glahn DC, Fox PT (2009) Investigating the functional heterogeneity of the default mode network using coordinate-based meta-analytic modeling. J Neurosci 29:14496–14505.

Laird AR, Eickhoff SB, Rottschy C, Bzdok D, Ray KL, Fox PT (2013) Networks of task co-activations. Neuroimage 80:505–514.

Lambon-Ralph M, Jefferies E, Patterson K, Rogers TT (2017) The neural and computational bases of semantic cognition. Nat Rev Neurosci 18:42–55.

Leech R, Kamourieh S, Beckmann CF, Sharp DJ (2011) Fractionating the default mode network: distinct contributions of the ventral and dorsal posterior cingulate cortex to cognitive control. J Neurosci 31:3217–3224.

Liu X, Li H, Luo F, Zhang L, Han R, Wang B (2015) Variation of the default mode network with altered alertness levels induced by propofol. Neuropsychiatr Dis Treat 11:2573–2581.

Lyu B, Choi HS, Marslen-Wilson WD, Clarke A, Randall B, Tyler LK (2019) Neural dynamics of semantic composition. Proc Natl Acad Sci USA 116:21318–21327.

Margulies DS, Ghosh SS, Goulas A, Falkiewicz M, Huntenburg JM, Langs G, Bezgin G, Eickhoff SB, Castellanos FX, Petrides M, Jefferies E, Smallwood J (2016) Situating the default-mode network along a principal gradient of macroscale cortical organization. Proc Natl Acad Sci USA 113:12574–12579.

Marreiros AC, Kiebel SJ, Friston KJ (2008) Dynamic causal modelling for fMRI: a two-state model. Neuroimage 39:269–278.

Monosov IE (2017) Anterior cingulate is a source of valence-specific information about value and uncertainty. Nat Commun 8:134.

Murphy K, Birn RM, Handwerker DA, Jones TB, Bandettini PA (2009) The impact of global signal regression on resting state correlations: are anti-correlated networks introduced? Neuroimage 44:893–905.

Pappas I, Craig MM, Menon DK, Stamatakis EA (2020) Structural optimality and neurogenetic expression mediate functional dynamics in the human brain. Hum Brain Mapp 41:2229–2243.

Perri CD, Bahri MA, Amico E, Thibaut A, Heine L, Antonopoulos G, Charland-Verville V, Wannez S, Gomez F, Hustinx R, Tshibanda L, Demertzi A, Soddu A, Laureys S (2016) Neural correlates of consciousness in patients who have emerged from a minimally conscious state: a cross-sectional multimodal imaging study. Lancet Neurol 15:830–842.

Pessoa L (2008) On the relationship between emotion and cognition. Nat Rev Neurosci 9:148–158.

Raichle ME (2015) The brain's default mode network. Annu Rev Neurosci 38:433–447.

Raichle ME, MacLeod AM, Snyder AZ, Powers WJ, Gusnard DA, Shulman GL (2001) A default mode of brain function. Proc Natl Acad Sci USA 98:676–682.

Seeley WW, Menon V, Schatzberg AF, Keller J, Glover GH, Kenna H, Reiss AL, Greicius MD (2007) Dissociable intrinsic connectivity networks for salience processing and executive control. J Neurosci 27:2349–2356.

Seghier ML (2013) The angular gyrus: multiple functions and multiple subdivisions. Neuroscientist 19:43–61.

Smith SM, Fox PT, Miller KL, Glahn DC, Fox PM, Mackay CE, Filippini N, Watkins KE, Toro R, Laird AR, Beckmann CF (2009) Correspondence of the brain's functional architecture during activation and rest. Proc Natl Acad Sci USA 106:13040–13045.

Smith V, Duncan J, Mitchell DJ (2021) Roles of the default mode and multiple-demand networks in naturalistic versus symbolic decisions. J Neurosci 41:2214–2228.

Sotiropoulos SN, Jbabdi S, Xu J, Andersson JL, Moeller S, Auerbach EJ, Glasser MF, Hernandez M, Sapiro G, Jenkinson M, Feinberg DA, Yacoub E, Lenglet C, Van Essen DC, Ugurbil K, Behrens TEJ; WU-Minn HCP Consortium (2013) Advances in diffusion MRI acquisition and processing in the Human Connectome Project. Neuroimage 80:125–143.

Spreng RN, DuPre E, Selarka D, Garcia J, Gojkovic S, Mildner J, Luh W-M, Turner GR (2014) Goal-congruent default network activity facilitates cognitive control. J Neurosci 34:14108–14114.

Stephan KE, Penny WD, Daunizeau J, Moran RJ, Friston KJ (2009) Bayesian model selection for group studies. Neuroimage 46:1004–1017.

Stephan K, Penny W, Moran R, den Ouden H, Daunizeau J, Friston K (2010) Ten simple rules for dynamic causal modeling. Neuroimage 49:3099–3109.

Tomasi D, Volkow ND (2011) Functional connectivity hubs in the human brain. Neuroimage 57:908–917.

Tops M, Boksem MAS, Quirin M, IJzerman H, Koole SL (2014) Internally directed cognition and mindfulness: an integrative perspective derived from predictive and reactive control systems theory. Front Psychol 5:429.

Utevsky AV, Smith DV, Huettel SA (2014) Precuneus is a functional core of the default-mode network. J Neurosci 34:932–940.

van den Heuvel MP, Sporns O (2011) Rich-club organization of the human connectome. J Neurosci 31:15775–15786.

van den Heuvel MP, Sporns O (2013) Network hubs in the human brain. Trends Cogn Sci 17:683–696.

Van Essen DC, Ugurbil K, Auerbach E, Barch D, Behrens TEJ, Bucholz R, Chang A, Chen L, Corbetta M, Curtiss SW, Della Penna S, Feinberg D, Glasser MF, Harel N, Heath AC, Larson-Prior L, Marcus D, Michalareas G, Moeller S, Oostenveld R, et al. (2012) The Human Connectome Project: a data acquisition perspective. Neuroimage 62:2222–2231.

Van Essen DC, Smith SM, Barch DM, Behrens TEJ, Yacoub E, Ugurbil K; WU-Minn HCP Consortium (2013) The WU-Minn Human Connectome Project: an overview. Neuroimage 80:62–79.

Vanhaudenhuyse A, Noirhomme Q, Tshibanda LJF, Bruno MA, Boveroux P, Schnakers C, Soddu A, Perlbarg V, Ledoux D, Brichant J-F, Moonen G, Maquet P, Greicius MD, Laureys S, Boly M (2010) Default network connectivity reflects the level of consciousness in non-communicative brain-damaged patients. Brain 133:161–171.

Vatansever D, Menon DK, Manktelow AE, Sahakian BJ, Stamatakis EA (2015) Default mode network connectivity during task execution. Neuroimage 122:96–104.

Vatansever D, Menon DK, Stamatakis EA (2017) Default mode contributions to automated information processing. Proc Natl Acad Sci USA 114:12821–12826.

Weissman DH, Roberts KC, Visscher KM, Woldorff MG (2006) The neural bases of momentary lapses in attention. Nat Neurosci 9:971–978.

Whitfield-Gabrieli S, Nieto-Castanon A (2012) Conn: a functional connectivity toolbox for correlated and anticorrelated brain networks. Brain Connect 2:125–141.

Woo CW, Krishnan A, Wager TD (2014) Cluster-extent based thresholding in fMRI analyses: pitfalls and recommendations. Neuroimage 91:412–419.

Yarkoni T, Poldrack RA, Nichols TE, Van Essen DC, Wager TD (2011) Large-scale automated synthesis of human functional neuroimaging data. Nat Methods 8:665–670.

Zeidman P, Jafarian A, Corbin N, Seghier ML, Razi A, Price CJ, Friston KJ (2019) A guide to group effective connectivity analysis, part 1: first level analysis with DCM for fMRI. Neuroimage 200:174–190.

Zhang S, Li CS (2012) Functional connectivity mapping of the human precuneus by resting state fMRI. Neuroimage 59:3548–3562.